J Mater Sci (2011) 46:1714–1722
DOI 10.1007/s10853-010-4989-z

Effect of thermal treatment on hardness and fracture toughness of a poly-*para*-phenylene-copolymer

K. Friedrich · A. A. Almajid · A. Noll · T. Burkhart

Received: 28 June 2010 / Accepted: 6 October 2010 / Published online: 30 October 2010

Abstract Up to now, poly-*para*-phenylene (PPP) can be considered as the stiffest and strongest polymer under ambient temperature conditions. As an amorphous thermoplastic, a thermal treatment will not change the material's morphology, but may influence its inner free volume (physical aging) and corresponding mechanical properties. This was investigated in this study with regard to the hardness and fracture toughness of PPP. It turned out that under the thermal conditions chosen, only moderate effects on these properties could be detected. Besides it was of interest how PPP compares in these properties relative to other advanced thermoplastics (neat and short glass fiber reinforced). Various features, such as striations and parabolic holes, on the fracture surfaces of PPP were also discussed.

Introduction

Poly-*para*-phenylene-copolymer (PPP) is a relatively new, amorphous thermoplastic, which is based on very stiff poly-(4,1-phenylene)-structured polymer chains [1–3]. At each phenylene ring, special substitutes are attached, which allow this material to become more flexible. In other words, the stiff molecular backbone provides high strength and modulus to the system, while the substituents lead to a better processibility, e.g. by compression molding or extrusion into simple part geometries (Fig. 1).

At present, this self-reinforcing polymer can be considered to be (at room temperature) the stiffest and strongest polymer world wide (i.e. without an additional type of reinforcement, such as short glass or carbon fibers). Preliminary studies at room temperature have resulted in a tensile strength of 207 MPa, a tensile modulus of 8.3 GPa (i.e. much higher than e.g. polyetheretherketone (PEEK), with 3.65 GPa), and a compressive strength of >620 MPa, all at a density of 1.21 g/cm^3. In terms of the specific strength (tensile strength/density), PPP exceeds clearly the corresponding values of general purpose construction steel or of typical aluminum alloys (Fig. 2).

According to these values, it can be expected that this material has also exceptional properties under other loading conditions. Of particular interest in this study was the resistance of this material against (a) penetration by a sharp indenter (representing the hardness of the polymer), and (b) crack propagation (representing the polymer's fracture toughness). In addition, the effect of different thermal treatments on these properties should be investigated.

Experimental

Materials

Poly-*para*-phenylene-copolymer (PPP) from two different suppliers was available for this study. The company Ensinger, Germany, provided extruded rods (Tecamax SRP), having a diameter of 3 cm, from which test samples were produced by machining (in the following designated as PPP (E)). They were compared with specimens taken from 1.5 cm thick, extruded plates, which were delivered

K. Friedrich (✉) · A. Noll · T. Burkhart
Institute for Composite Materials (IVW GmbH), Technical University of Kaiserslautern, 67663 Kaiserslautern, Germay
e-mail: Klaus.Friedrich@ivw.uni-kl.de

K. Friedrich · A. A. Almajid
CERAM, College of Engineering, King Saud University, Riyadh, Saudi Arabia

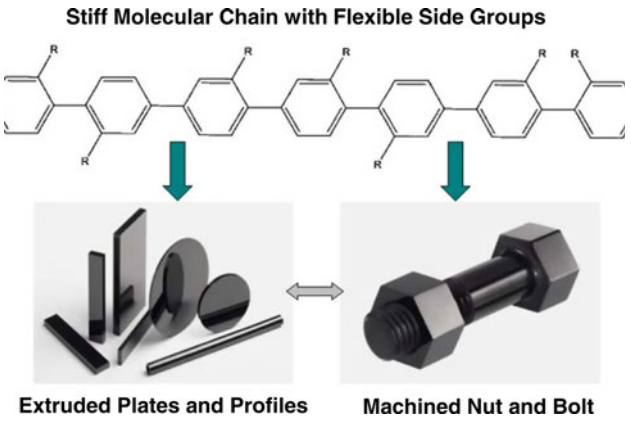

Fig. 1 PPP chain structure and products

by the company Solvay Advanced Polymers, USA (Primospire PR 120, in the following designated as PPP (S)).

Thermal treatments

Small plates of material PPP (S), having a width of 40 mm, a length of 48 mm, and a thickness of 6.8 mm, were embedded in a closed steel mold (Fig. 3). During the first treatment, the mold with the sample inside was put in an oven, having an air temperature of 220 °C inside. This temperature exceeded clearly the glass transition (melting) temperature of the polymer, which was determined to be the in range between 157 and 167 °C [4]. After a period of 4 h, the mold was quenched in cold water, so that the polymer inside reached room temperature within a minute or less. The samples were designated as "quenched" (Q) in that what follows (Fig. 4).

The second treatment consisted of the heating and quenching procedure, described before, and a subsequent annealing process by exposing the mold (with the polymer plates inside) to a temperature of 125 °C in another oven over a period of 3 h, followed by rapid cooling in water. This treatment was called "annealed" (AN).

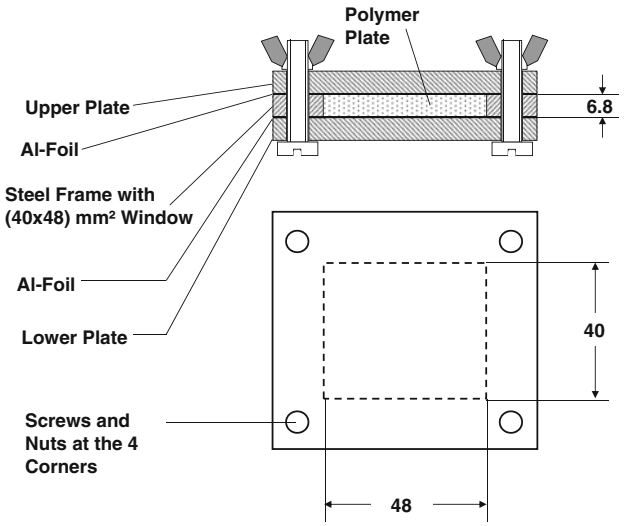

Fig. 3 Mold for thermal treatment of PPP

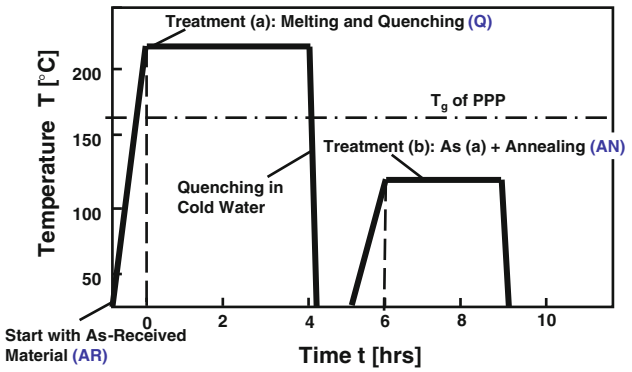

Fig. 4 Thermal treatments of PPP for comparison to the "as received" (AR) material

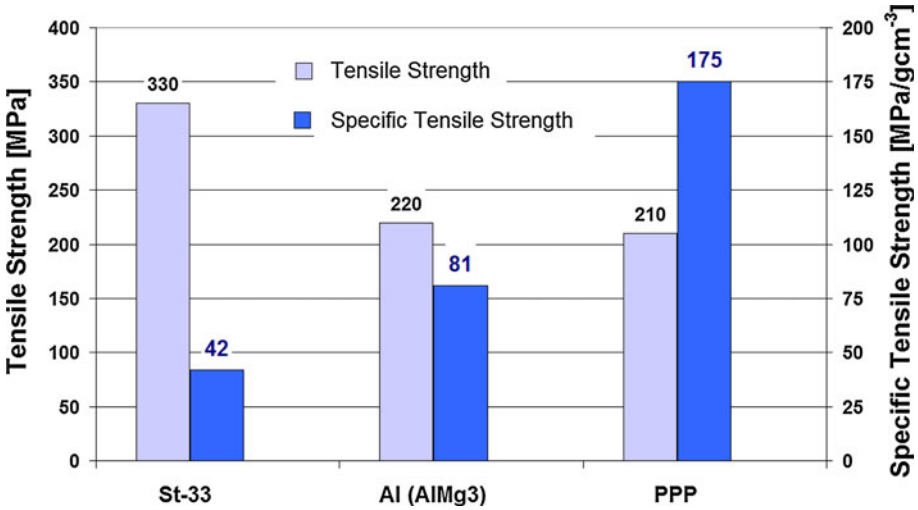

Fig. 2 Absolute and specific tensile strength of PPP versus steel and an aluminum alloy

Hardness measurement

The Martens hardness HM of the "as received" (AR) and the differently treated materials was determined by the use of a Dynamic Ultra Micro Hardness Tester, DUH-202, Shimadzu Corp., Japan. A Vickers diamond indenter was pressed onto a flat surface of each sample, until a complete load-penetration depth-curve was achieved. Figure 5 compares such curves for the materials PPP (E) and PEEK 450G. The hardness of PPP is almost 2 times higher than the hardness of PEEK. From these curves, also a rough calculation of the elastic modulus can be derived by looking at the tangent of upper part of the load release branch of these curves [5, 6]. This resulted in a value of ca. 9300 MPa for PPP and a value of 4200 MPa for PEEK, confirming more or less the data from the literature and the corresponding DMTA-tests [4].

Fracture toughness tests

Due to the different geometry of the intermediate material forms, delivered by the two companies, the shape of the samples used for determining the materials resistance against crack propagation (critical stress intensity factor or fracture toughness K_{IC}) was also different. In case of PPP (E), single edge notched tensile (SEN) specimens were used, whereas the values for the differently treated PPP (S) materials were determined with a compact tension (CT) test geometry (Fig. 6). In both cases, it was attempted to create a sharp crack in the root of the machined notch by the use of a fresh razor blade (which was not always easy and perfect, due to the very high hardness of PPP). Loading was carried out on a universal tensile testing machine (Zwick, Germany), at room temperature environment and a loading speed of 0.1 mm/min. From the corresponding load displacement curves (Fig. 7), K_{IC} was calculated by using the following formula:

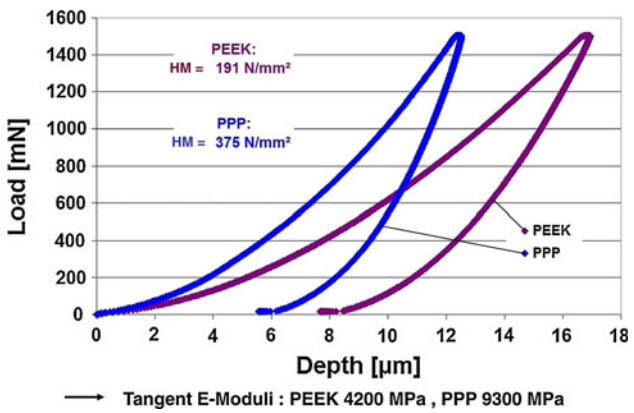

Fig. 5 Typical load–depth-curves for determining the Martens hardness of polymers (here: PPP versus PEEK)

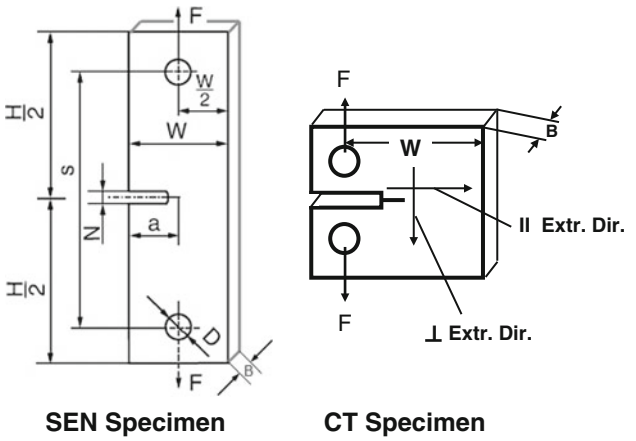

Fig. 6 Configuration of specimens for fracture toughness testing: *left* single edge notch (SEN) specimen, as used for Ensinger material ($W = 20$ mm; $B = 3$ mm); *right* compact tension (CT), as used for Solvay material ($W = 37$ mm; $B = 6.8$ mm). In both cases, F refers to the applied load

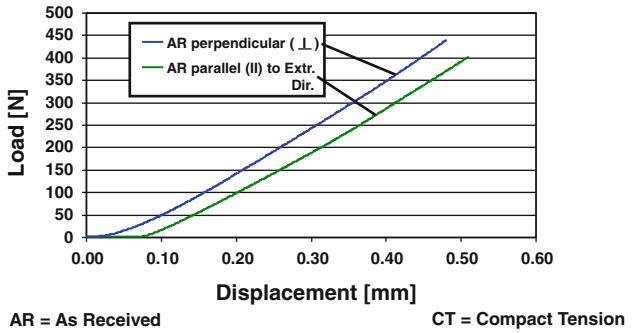

Fig. 7 Load–displacement curves for CT specimens loaded with a crack either parallel or perpendicular to the extrusion direction of AR-PPP material

$$K_{IC} = F_{max}/(B * W) * f(a/W),$$

where F_{max} is the maximum load at break, B is the thickness of the sample, W is the width of the sample, and $f(a/W)$ is a geometrical correction factor, as given for different test geometries in the literature [6]. It should be mentioned, however, that the geometry of the samples used here was not in exact agreement with the ones recommended by different standards. Therefore, the values can only be considered for comparison between the different materials and treatments, but not as 100% absolute standard values for the polymer PPP.

Fracture surface analysis

Scanning electron microscopy (SEM)

An ultra high resolution field emission scanning electron microscope (FESEM) (Carl Zeiss SMT AG, SUPRA^{TM}

40VP, Germany), was used to observe the fracture surfaces, operating with 10 kV acceleration voltage, a working distance of less than 10 mm, and a secondary electron detector. Therefore, the respective surface was sputter-coated for 70 s with gold.

Furthermore, energy dispersive X-ray spectroscopy (EDX) analyses (Noran System Six, Thermo Scientific, Germany, linked with FESEM) were conducted at 15 kV and a magnification of 20,000 fold to observe material composition of impurities, which were found on the facture surfaces.

Atomic force microscopy (AFM)

Atomic force microscopy (AFM) examinations were carried out to get real space topographical images, height information of the fracture surfaces, and a correlation to FESEM observations. In this study, a MultiMode, Veeco Instruments GmbH, Germany, were applied in tapping mode, using an Si cantilever with a resonance frequency of 300 kHz. The height and amplitude signals were utilized to visualize the structures of the fracture surfaces.

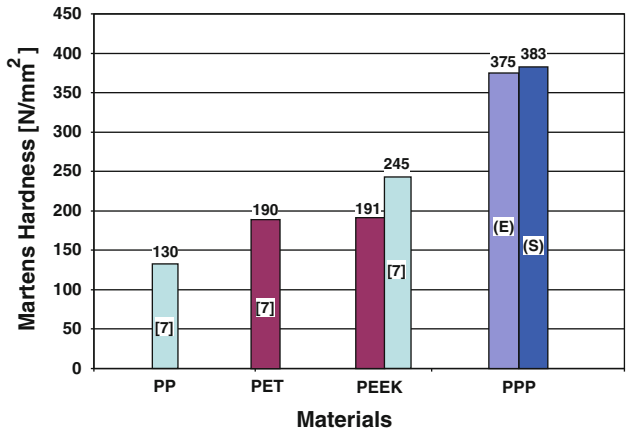

Fig. 8 Comparison of Martens hardness of various PPP's versus PEEK, PET, and PP. Columns indicated with [7] were taken from this literature reference, whereas the rest is based on own measurements

Results and discussion

Hardness

According to Fig. 5, PPP has, in general, a hardness which is twice as high as that of PEEK. It is also superior to other high performance polymers [7], as shown in Fig. 8. Here it is also shown that there is practically no difference in hardness between the two PPP grades, received from Ensinger and Solvey.

Looking at PPP in more detail, it becomes evident that the as received plates from Solvey (PPP (S)) exhibit a little anisotropy in the hardness values due to the orientation of the stiff molecules during the extrusion process (Fig. 9).

When considering the effect of the heat treatment, this anisotropy effect disappeared. The re-melting and quenching operation (Q) caused a random orientation of stiff molecules, associated with a moderate softening of the whole morphology. This was combined with a slight reduction of the hardness values (Fig. 9). The subsequent annealing process of the quenched material (AN), which can also be considered as a physical aging, resulted, in turn, in a rather small increase in hardness due to a compaction of the amorphous structure. This is also well known from other amorphous polymers [8, 9].

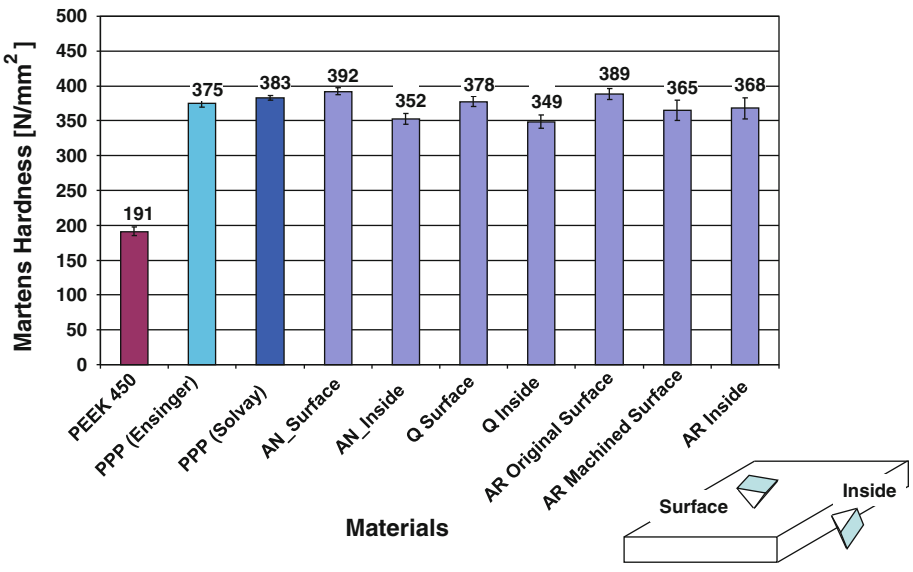

Fig. 9 Martens hardness of PPP as a function of thermal treatment and position of indentation

Fracture toughness

In a general comparison with other thermoplastics, the fracture toughness of the as-received PPP lies in an intermediate range. It is more brittle than the very tough PEEK, but tougher than the rather brittle polyphenylenesulfide (PPS). Figure 10 summarizes the toughness values of PPP (from the two suppliers), as well as neat and short glass fiber (SGF) reinforced polyetheretherketone (PEEK) [10], PPS [11], polyethyleneterephthalate (PET) [12], liquid crystal polymer (LCP) [13], polyamide (PA 66) [14], and (a low molecular weight) polypropylene (PP) [15]. Although the various materials were tested under slightly different conditions, the data give an impression of what can be expected from PPP in comparison to other neat and short fiber reinforced thermoplastics.

The small anisotropy already observed for the as received PPP (S) in case of the hardness is also reflected in the fracture toughness values. CT specimens with a starter crack parallel to the extrusion direction of the plates exhibited slightly lower K_{IC}-values than those with a crack perpendicular to the extrusion direction. This means, a preferred molecular orientation transverse to the initial crack direction results in a greater resistance against crack propagation (Fig. 11). However, when it comes to the heat-treated samples, the anisotropy in fracture toughness does not exist any more. At the same time, the fracture toughness of the quenched samples exceeded clearly the one of the AR-samples with cracks parallel to the extrusion direction. This means a more random molecular orientation in a sample, containing simultaneously less internal stresses than the extruded ones, results in higher fracture toughness. Also here, a subsequent physical aging, respectively, annealing (AN), of the quenched PPP-samples resulted again in an increase of the brittleness of the materials, as reflected in a lower K_{IC}-value compared to the Q-samples (Fig. 11). This is in accordance with the observations made from the hardness values.

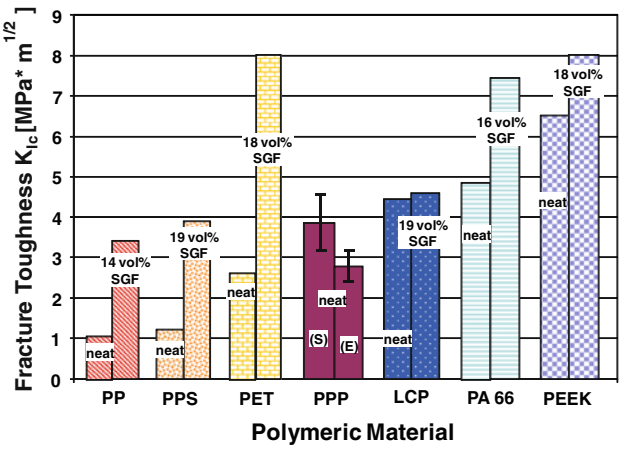

Fig. 10 Fracture toughness of PPP in comparison to other unreinforced and short glass fiber reinforced thermoplastics. Plot in the order of increasing K_{Ic} of the neat matrices! In the reinforced samples, cracks were run transverse to the mold filling direction of the injection molded plates. Differences between PPP (S) and PPP (E) are most probably due to the quality of pre-cracking, other manufacturing procedures of the starting materials, and different specimen geometries

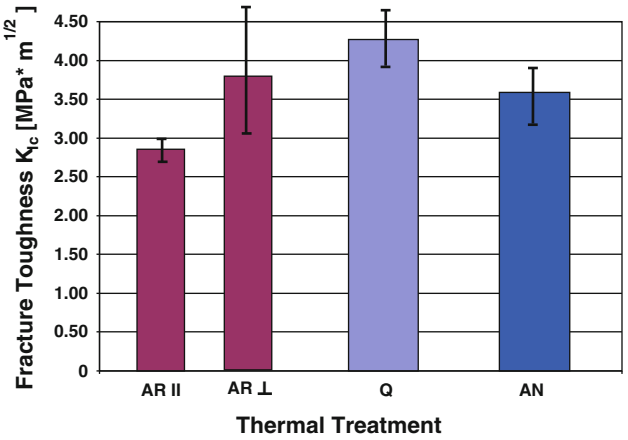

Fig. 11 Influence of thermal treatment and crack direction on fracture toughness of PPP

Analysis of the fracture surfaces

Figure 12 is a low magnification SEM-micrograph of one of the fracture surfaces, illustrating the difficulty to produce a uniform razor crack, emanating from the machined notch. The razor crack looks slightly curved, it is not existent over the total thickness of the sample, and due to local damage sites of the razor blade as a result of its pressing into the hard polymer, the real fracture surface starts with rather rough features behind the razor crack. Therefore, the resulting K_{IC}-values can only be considered as relative values allowing a distinction between the different thermal treatments.

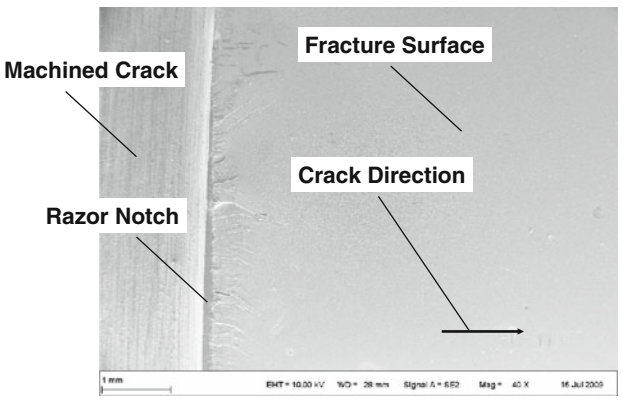

Fig. 12 Fracture surface of PPP: overview with razor notch

A higher magnification of the fracture surfaces (Fig. 13) in case of the AR-material shows a uniform striation pattern as it is known from other amorphous thermoplastics [16]. These patterns are an evidence for very fast crack propagation, especially when the materials are rather brittle. Each striation has a rough appearance at the beginning followed by a smoother part, until the next striation is formed. Going even to higher magnifications illustrates that the failure of the polymer in the different regions of the striations occurs by the rupture of individual molecular bundles, indicated on the fracture surface by stretched features with a white tip at the end (Fig. 14 see arrow). Similar observations have been made in the past by people who have investigated the craze fracture phenomena in PMMA [17].

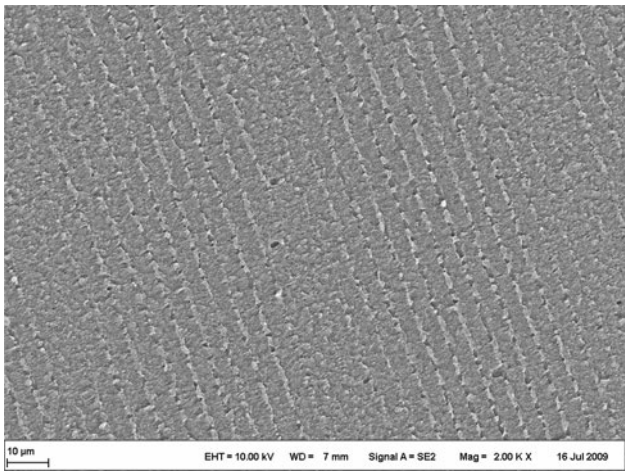

Fig. 13 Striation pattern on the fracture surface of as received PPP: striation width ca. 5.3 µm

In addition, there have been quite some publications in the past on high performance, highly ductile thermosetting polymers. An overview gives the book on "polymer toughening", edited by Arends [18]. Some of the fracture features observed here, e.g. the debonding of the matrix around less-compliant sub-micrometer particles (Fig. 15), have also been reported by Sue et al. [19] for aliphatic polyketons, often associated with crazing phenomena, even in high performance thermosetting resins [20, 21]. One can get tough or ductile epoxies also by controlling the molecular structures. The group around Mai and co-workers [22, 23] has been working on nanostructured epoxies, whereby they used di-block or tri-block copolymers to react with epoxies so that one block is miscible with epoxy and other block is not. In this way, they could get nanostructures with spheres, worm-like, etc. whose toughness was dependant on these features. Others use chain extenders or flexible amines to increase ductility and toughness of epoxies; or even controlling epoxy network deformation [24–26].

Back to the present case, the appearance of the fracture surfaces changes a bit when looking at the Q-samples. The striations are almost not visible at the beginning of the fracture surface, but only show up at the very far end of the broken sample. This is an indication for a slower fracture propagation, due to a slightly higher toughness of the polymer in this state (Fig. 15). Under this condition, the fracture surface shows several lager holes in between of the rest of the fracture surface. A closer look into these holes gives evidence that there are sites of secondary crack formation in front of the main crack front, as a result of minor Zn or ZnO impurities in the PPP. This could be detected by the use of an EDX-device, linked to the SEM-facility used (Fig. 16). It was unfortunate that (due to a present lack of

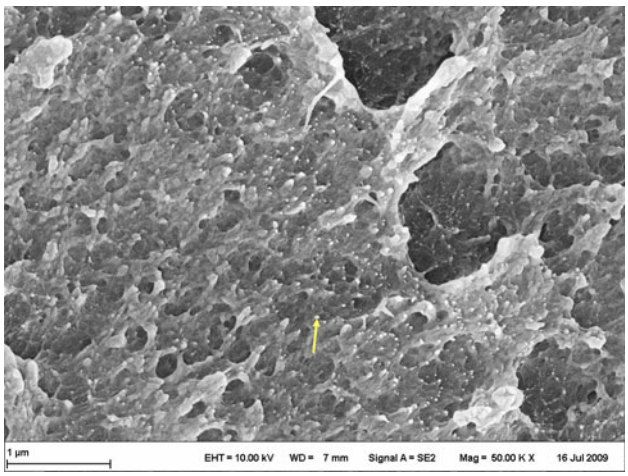

Fig. 14 Higher magnification of a striation on the fracture surface of as received PPP

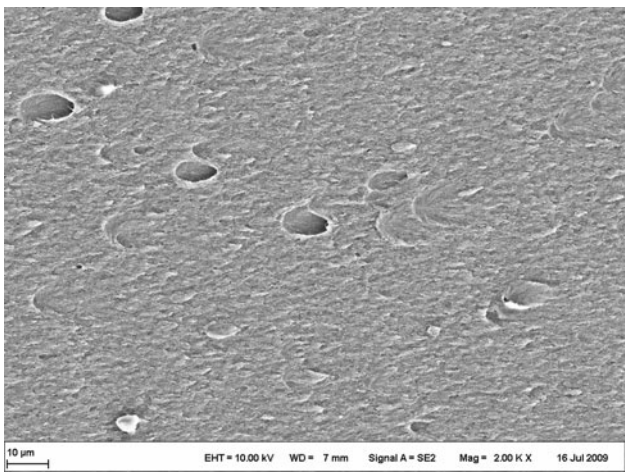

Fig. 15 Smoother appearance with local holes and parabolic features on the fracture surface of quenched PPP

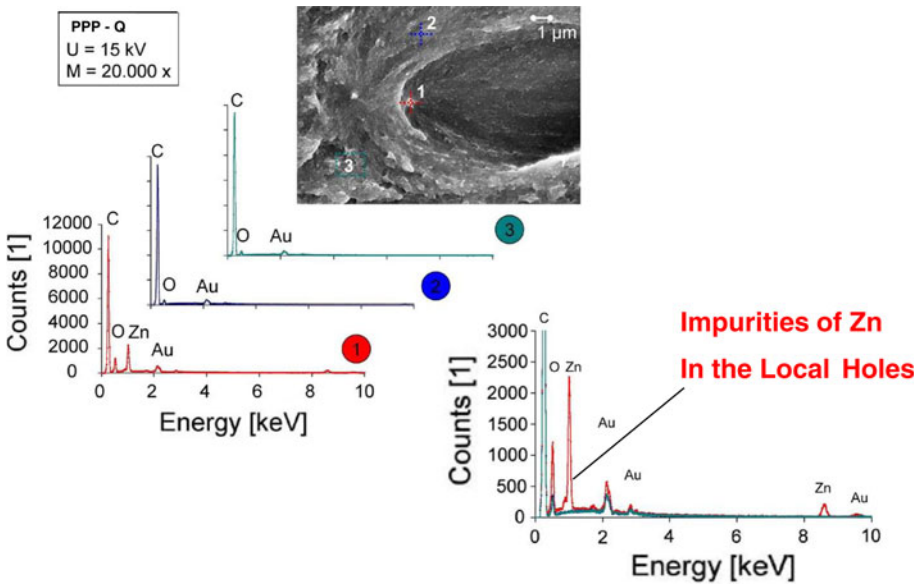

Fig. 16 EDX analysis of fracture surface of PPP after treatment Q, showing Zn containing impurities in the local holes

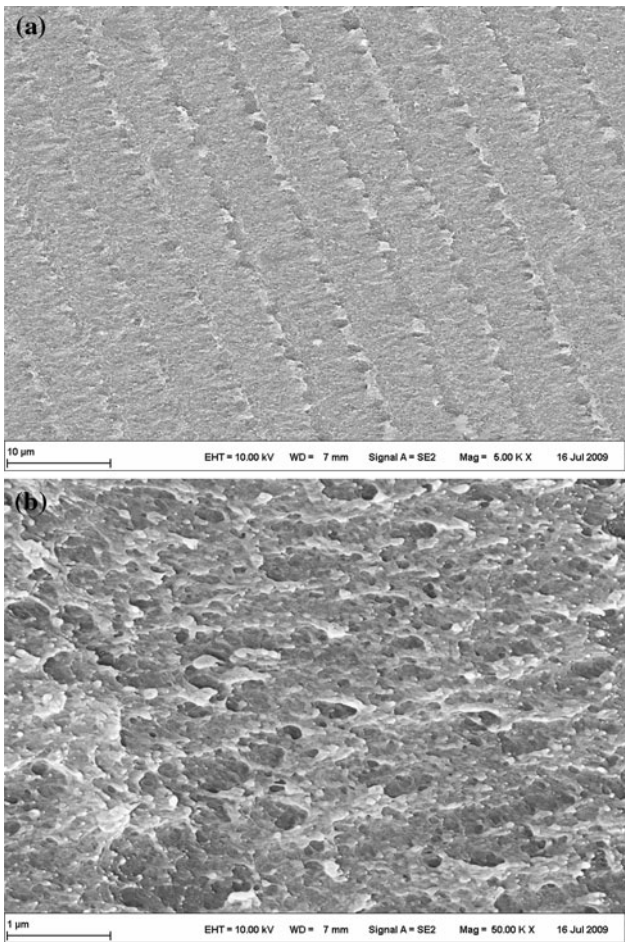

Fig. 17 Striation pattern on the fracture surface of PPP after treatment AN (**a**), and higher magnification of the stretched molecular bundles in the smoother part of the striations (**b**)

equipment) no transmission electron microscopy (TEM) could be performed for investigating more details of the PPP morphology. This might have shed more light on the observed fracture behavior. However, future works on other PPP's will probably also show TEM details of the Zn-containing particles and their distribution.

As expected from the fracture toughness tendencies, an SEM-check of the AN-samples showed a similar appearance as the AR-samples, i.e. striations over the whole range of the fracture surface and the rupture of molecular bundles at higher magnification (Fig. 17a, b). The latter features were, of course, also observed when looking at the Q-samples under higher magnification.

Finally, further details of the fracture surface features can be detected from AFM pictures taken in different modes. Using the height information (Fig. 18) allows to estimate the differences in surface roughness at the beginning of each striation and within its smoother region. Each striation starts with a rough region, having height differences up to 1000 nm, whereas the major part of the striations is within a narrow range of around 100 nm. This can be seen indirectly also under amplitude contrast, reflecting hills and holes next to each other at the beginning of each striation (Fig. 19). The width of the striations in case of the AR-samples amounts to ca. 5 µm, which is in agreement with the measurements taken from the SEM micrographs.

Conclusions

Poly-*para*-phenylene-copolymer is an amorphous thermoplastic, which has at room temperature the highest strength,

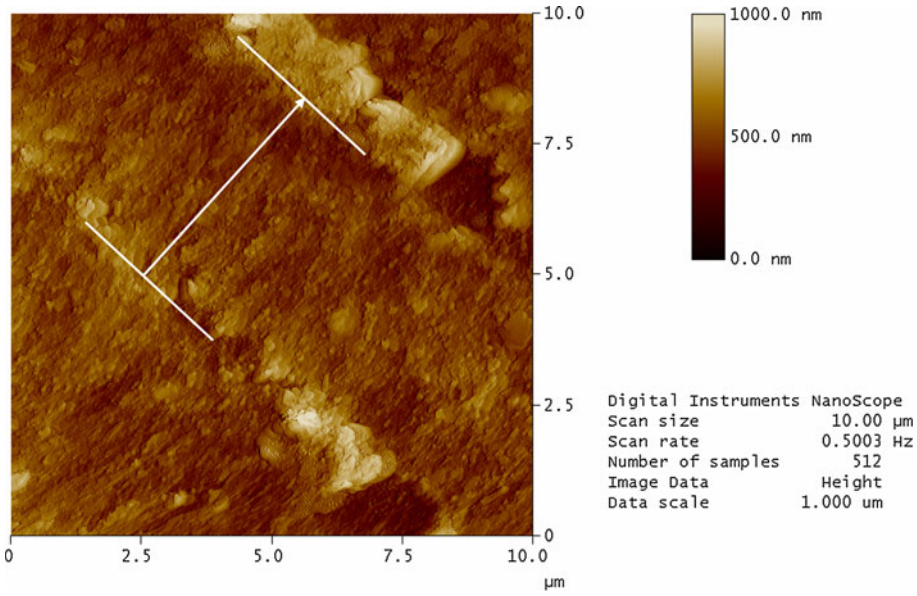

Fig. 18 Height contrast AFM picture of a striation on the fracture surface of the as received PPP. The *white arrow* indicates the direction of crack propagation within each striation

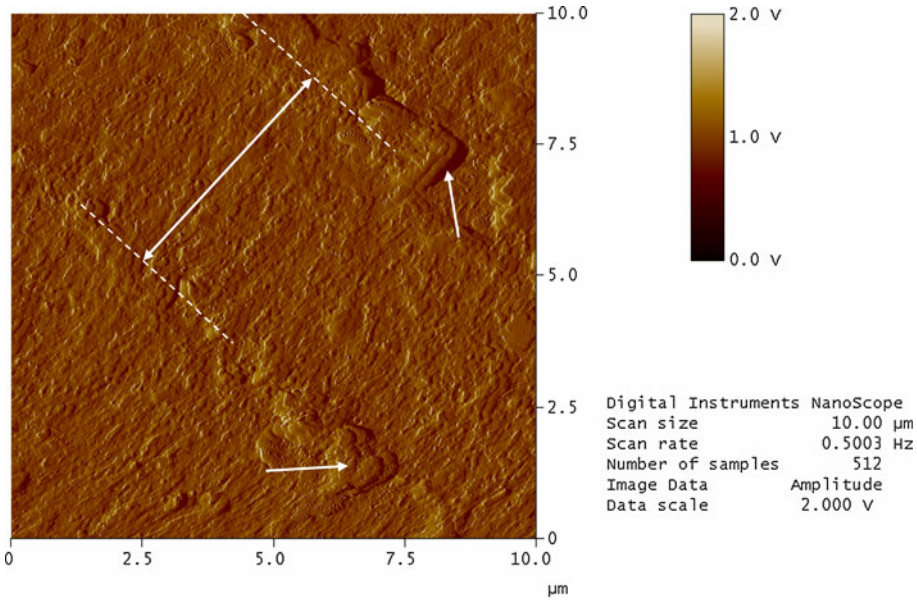

Fig. 19 AFM amplitude contrast of the same location as Fig. 18 (striation width ca 5.4 µm), indicating deep holes and hills at the beginning of each striation (*arrows*)

stiffness, and hardness of all polymers currently available. Looking at its mechanical performance as a function of thermal treatment (as received versus melting and quenching verus melting, quenching, and annealing) resulted in the following differences:

(a) The as received, extruded material exhibited a slight anisotropy in hardness and toughness due to a minor orientation of the stiff molecules during the extrusion process.
(b) The anisotropy disappeared after the two thermal treatments.
(c) The melting/quenching treatment resulted in slightly lower values of hardness, but higher values in toughness.
(d) After subsequent annealing, the material went, on average, back to its original state after extrusion, which seems to be a result of a physical aging process (densification of the amorphous structure).
(e) The striation pattern on the fracture surfaces is an interesting phenomenon, and its origin should be investigated in more detail in the future.

Acknowledgements The authors are grateful to the companies Solvay Advanced Polymers, USA, and Ensinger GmbH, Germany, for kindly supplying the materials. Further thanks are due to the King Saud University, Riyadh, Saudi Arabia, for the financial support of the collaboration between the two institutes. The help of Mr. S. Schmitt and Mr. R. Schimmele (both IVW) in performing hardness, AFM and fracture toughness tests is also gratefully acknowledged.

References

1. Malkovich N, Gané R (2005) Mississippi Polymer Technologies Inc., Presentation to NDIA, May 17, 2005
2. NN (2005) Tecamax SRP-Extreme Festigkeit ohne Faserverstärkung, Ensinger GmbH, Germany, Produkt information
3. NN (2007) PrimoSpire self-reinforced polyphenylene, Solvay Advanced Polymers, USA, Product Information
4. Friedrich K, Burkhart T, Almajid AA, Haupert F (2010) Int J Polym Mater 59:680
5. Oliver WC, Pharr GM (1992) J Mater Res 7:1564
6. Grellmann W, Seidler S (eds) (2007) Polymer testing. Hanser, München
7. Koch T, Seidler S (2009) Strain 45:26
8. Bárány T, Czigány T, Karger-Kocsis J (2010) Prog Polym Sci 35:1257
9. Hay JN (1995) Pure Appl Chem 67:1855
10. Friedrich K, Walter R, Voss H, Karger-Kocsis J (1986) Composites 17:205
11. Karger-Kocsis J, Friedrich K (1987) J Mater Sci 22:947. doi:10.1007/BF01103535
12. Friedrich K (1985) Compos Sci Technol 1:43
13. Voss H, Friedrich K (1986) J Mater Sci 21:2889. doi:10.1007/BF00551508
14. Karger-Kocsis J, Friedrich K (1988) Compos Sci Technol 32:293
15. Spahr DE, Friedrich K, Bailey RS, Schultz JM (1990) J Mater Sci 25:4427. doi:10.1007/BF00581104
16. Friedrich K (1977) J Mater Sci Lett 12:640
17. Döll W (1983) Adv Polym Sci 52(53):105
18. Arends C B (ed) (1996) Polymer toughening. Marcel Dekker, New York, USA
19. Lu J, Li CK-Y, Wei G-Y, Sue H-J (2000) J Mater Sci 35:271. doi:10.1023/A:1004724730058
20. Sue H-J, Garcia-Meitin EI, Yang PC, Bishop MT (1977) J Mater Sci 12:1463. doi:10.1007/BF00540863
21. Sue H-J (2001) In: Buschow K-HJ, Cahn RW, Flemings MC, Ilschner B, Kramer EJ, Mahajan S, Veyssiere P (eds) Encyclopedia of materials: science and technology. Elsevier, Amsterdam, The Netherlands, p 6113
22. Xi ZG, Hameed N, Guo QP, Mai Y-W (2010) J Appl Polym Sci 115:2110
23. Hameed N, Guo QP, Hanley T, Mai Y-W (2010) J Polym Sci B 48:790
24. Blance M, Lopez M, De Arxaya PA, Ramos JA, Kortaberria G, Riccardi CC, Mondragon I (2009) J Appl Polym Sci 114:1753
25. Kuan H-C, Dai J-B, Ma J (2010) J Appl Polym Sci 115:3265
26. Yang G, Fu S-Y, Yang J-P (2007) Polymer 48:302